CONSISTENT ESTIMATION OF THE HEMODYNAMIC RESPONSE FUNCTION IN FNIRS

Adnan Shah[1] *and Abd-Krim Seghouane*[2]

[1] NICTA and The ANU College of Engineering and Computer Science, Canberra.
[2] Department of Electrical and Electronic Engineering, Melbourne School of Engineering,
The University of Melbourne. [1] {adnan.shah@anu.edu.au}, [2] {abd-krim.seghouane@unimelb.edu.au}

ABSTRACT

Non-parametric hemodynamic response function (HRF) estimation in noisy functional near-infrared spectroscopy (fNIRS) plays an important role when investigating the temporal dynamics of a brain region response during activations. Assuming the drift Lipschitz continuous; a new algorithm for non-parametric HRF estimation from the oxygenated (HbO) and deoxygenated (HbR) fNIRS time-series is derived in this paper. The proposed algorithm estimates the HRF by applying a first order differencing to the fNIRS time series samples. It is shown that the proposed HRF estimator is $\sqrt{N}$ consistent. Its performance is assessed using both simulated and a real fNIRS data set obtained from a motor activity experiment. The application results reveal that the proposed HRF estimation method is efficient both computationally and in terms of accuracy.

Keywords: fNIRS, hemodynamic response function, first order differencing, consistent estimation.

1. INTRODUCTION

Functional near-infrared spectroscopy (fNIRS) is a unique in-vivo imaging technology that simultaneously measures the concentration changes of oxygenated (HbO) and deoxygenated (HbR) hemoglobin. It has shown great potential to analyze cognitive functions during ecologically valid paradigms as it offers a flexible environment for measuring functional brain activity [1]. It provides a balance between temporal and spatial resolution unlike in-the-field neuroimaging techniques such as fMRI and EEG. Furthermore, the independent observation of HbO and HbR in fNIRS measurements and access to their sum as total hemoglobin (HbT) better characterizes the governing mechanism of neuronal dynamics than the blood oxygen level-dependent (BOLD) fMRI signal alone [2].

Primary source of signal contrast in fNIRS measurements is HbO and HbR that are negatively correlated during neural activations [3] through a mechanism known as neurovascular coupling [4]. Increase in neuronal activity increases HbO and decreases HbR. The changes in tissue oxygenation associated with neural activity modulate the absorption and scattering of the infrared light through the brain tissue. In principle, HbO and HbR have different attenuation spectra with characteristic properties in the optical window of the near-infrared spectral range $680 - 900\ nm$ [5, 4]. Therefore, different characterizing wavelengths are used in the optical window in fNIRS to differentiate non-invasively between the two qualitative measures associated with the neural activity.

The HbO and HbR as a first approximation are modeled as a convolution of the experimental paradigm characterizing the stimulus by the hemodynamic response function (HRF), modeling the impulse response of the neurovascular system [6] that is assumed to be linear time-invariant [7].

HRF shape vary substantially across regions as is recently revealed by [8] in an fMRI study, apart from the understood notion of its variability across tasks and subjects. Therefore, accurate HRF estimation is essential to characterize the temporal dynamics of brain region response during activations, and the region involvement in functional and effective connectivity [9]. Based on generalized linear model (GLM), the available methods for HRF estimation from fMRI data can be adapted to fNIRS time-series [10]. Among them, parametric HRF estimation methods offer limited flexibity by a priori choosing a non-linear function of certain parameters that are estimated by least squares [11]. Nonparametric estimation methods allow more flexibility and offer accuracy in the estimation by inferring the HRF at each time sample [12].

Besides the noise, the estimation of the HRF is further complicated by the presence of drift arising from long term physiological effects and instrumental instability. Nonparametric methods introduced so far include a parametric part to infer the systematic drift, commonly modeled by polynomials and splines [13] and functions from the discrete cosine transform [12, 14]. However, the relatively un-restrained nature of fNIRS data acquisition system make it more tolerant of head motion than fMRI scanners giving rise to severe motion related artifacts that substantially degrade signal quality [1]. Effective HRF estimation requires a modeling approach that efficiently account for the variability of the baseline drift. Though the drift is considered as a nuisance component, its appropriate parametrization is needed for efficient HRF estimation.

In this paper, a nonparametric component is used to model the drift and a semiparametric model is used to describe the fNIRS responses [15]. Nonparametric regression models do not assume any a priori model structure and allows the representation of broad class of drift signals. Furthermore, they avoid the selection or the estimation of the nuisance covariates to approximate the drift.
Using the assumption that the drift is a superposition of physical and physiological effects that can be considered Lipschitz continuous, a $\sqrt{N}$ consistent HRF estimation procedure from the HbO and HbR fNIRS responses measured in a channel is proposed in this paper. This procedure is based on a first order differencing approach [16][17] applied to semiparametric model. Numerical performances of the proposed estimation procedure are illustrated on both simulated and real fNIRS data.

2. MODEL OF THE FNIRS SIGNAL

The HbO and HbR signals measured in channel C_i over the time course of N acquired samples during an fNIRS experiment can be represented by a discrete random sequence $\mathbf{y}_i = (y_{i1}, ..., y_{iN})^\top$. Each signal can be described as the sum of three components: an experimentally induced controlled activation response in channel i, an uncontrolled confound part or a baseline drift (including possible unknown nuisance effects) and a noise term [12, 14, 18]. In matrix form, fNIRS signal can be described with the following model

$$\mathbf{y}_i = X\theta_i + P\phi_i + \epsilon_i, \quad \epsilon_i \sim N(0, \sigma_\epsilon^2 I_N), \tag{1}$$

where X is a known $(N \times p)$ matrix representing the experimental design matrix consisting of the lagged stimulus covariates. The $(N \times q)$ drift matrix P, is a nuisance covariate matrix that takes a potential drift and any other nuisance effect into account. The elements of ϕ_i that are attached to each measured response in channel i are the corresponding coefficients. The parameter vectors θ_i and ϕ_i are unknown p and q dimensional vectors representing the unknown HRF samples to be estimated and the nuisance variables respectively. In practice the dimension q can be estimated using model selection techniques [19, 20, 21]. ϵ_i represents independent identically distributed Gaussian white noise $N(0, \sigma_\epsilon^2 I_N)$ with an unknown variance σ_ϵ^2.
The parametric component $P\phi_i$ is very useful for providing a parsimonious description of the baseline drift, but it is used at the risk of introducing a modeling bias. Alternatives that offer more flexibility in approximating the drift do exist, and can be obtained by using an unknown drift matrix P [18] or a nonparametric component [15]. The latter is used in this paper. In the matrix-vector form, the model of the fNIRS signal in this case is

$$\mathbf{y}_i = X\theta_i + \mathbf{f}_i + \epsilon_i, \tag{2}$$

where $\mathbf{f}_i = (f_i(t_1), ..., f_i(t_N))^\top$ is a discrete sequence independent of X representing the uncontrolled baseline drift including other unknown nuisance effects. Rescaling the experiment time to one shows that the spacing between two consecutive samples is of the order $\frac{1}{N}$.
In comparison to (1), model (2) does not require the parametrization of the baseline drift. It offers more flexibility than the linear model for representing the baseline drift while maintaining the explanatory power of the parametric model for the activation response measured in channel i.

3. PROPOSED HRF ESTIMATION PROCEDURE

In what follows, we propose a simple, but reliable and effective HRF estimation procedure. A first order difference-based estimate [16, 17] is used for estimating θ_i. For $j = 1, ..., N-1$

$$y_{i,j+1} - y_{i,j} = f_i(t_{j+1}) - f_i(t_j) + (X_{j+1} - X_j)\theta_i + e_{i,j}, \tag{3}$$

where the stochastic error $e_j = \epsilon_{j+1} - \epsilon_j$. Using the assumption that the drift is a superposition of instrumental and physiological effects that are Lipschitz continuous, we have the approximation

$$f_i(t_{j+1}) - f_i(t_j) \simeq O\left(\frac{1}{N}\right)$$

and

$$y_{i,j+1} - y_{i,j} \simeq (X_{j+1} - X_j)\theta_i + e_{i,j}. \tag{4}$$

In this case the least squares estimate of θ_i satisfies

$$\theta_i = \text{argmin}_{\theta_i} \sum_{j=1}^{N-1} \left(y_{i(j+1)} - y_{ij} - (X_{j+1} - X_j)\theta_i\right)^2 \tag{5}$$

and is given by

$$\hat{\theta}_i = \left(\sum_{j=1}^{N-1} (X_{j+1} - X_j)^\top (X_{j+1} - X_j)\right)^{-1} \cdot \sum_{j=1}^{N-1} (X_{j+1} - X_j)^\top (y_{i,j+1} - y_{i,j}) \tag{6}$$

The proposed HRF estimate (6) is $\sqrt{N}$ consistent. This is described in the Appendix. It is easily implementable and avoid the selection of nuisance covariates for modeling the baseline drift. Its effectiveness is guaranteed by the $\sqrt{N}$ consistency of $\hat{\theta}_i$ in (6).
While our focus is the HRF estimation θ_i, the proposed method also generates an estimation of the drift $\mathbf{f}_i$. Using the above HRF estimate $\hat{\theta}_i$, let

$$\mathbf{z}_i = \mathbf{y}_i - X\hat{\theta}_i. \tag{7}$$

Then, $\mathbf{z}_i = (z_{i1}, ..., z_{iN})^\top$ can be viewed as sampled from the model

$$\mathbf{z}_i \simeq \mathbf{f}_i + \epsilon_i. \quad (8)$$

This is a denoising problem in which we can employ a soft-thresholding technique to estimate $\mathbf{f}_i$ from $\mathbf{z}_i$ [22]. Since the convergence rate of $\hat{\theta}_i$ is faster than the wavelet shrinkage estimator [22], the errors in estimating θ_i are negligible when estimating $\mathbf{f}_i$.

4. RESULTS

4.1. Simulations

For simulating fNIRS time-series measurements, sixty time-series of 500-points each were simulated. For each time-series the stimulus sequence is a realization of a random event-related stimulus (random onsets arrival time), which is convolved with the original HRF θ_0 (canonical HRF used by SPM software [23]) that is normalized to one depicting HbO response. For negative correlated HbR response having smaller amplitude than HbO response [5], an inverted un-normalized HRF was considered for the same paradigm as shown in figure 1. Low frequency drifts $\mathbf{f}_0 = P\phi_i$ were added to both the simulated fNIRS time-series. The drift matrix P is an orthogonal matrix, which consists of orthonormal basis of functions generated from discrete cosine transform. The coefficients ϕ_i were drawn from a normal distribution, $N(0, 8.5)$. For generating the representative fNIRS drift in this simulation, the cosine basis were chosen covering Mayer waves (arterial blood pressure) centered around 0.1 Hz, head movement artifacts represented by basis in the range $[0.0038 \sim 0.015Hz]$, and respiration noise centered around 0.25 Hz [24]. These basis are linearly mixed with strength determined by weights from the drift coefficient vector ϕ_i. The dimension of the drift coefficients vector was kept to $q = 8$. The proposed method is compared with the ordinary least squares HRF estimator for different noise variances (σ_ϵ^2). Investigation of the HRF is assessed using the quadratic error as:

$$\eta_{\hat{\theta}_m} = \frac{1}{p-1} \parallel \hat{\theta}_m - \theta_0 \parallel^2$$

where $m \in \{\text{proposed, ordinary least squares}\}$ and θ_0 represents the true unknown HRF with p number of samples.

For a noise variance σ_ϵ^2 = 0.1, the quadratic-error for the proposed HRF estimator is 2.4 x 10^{-3} in comparison to 7.0 x 10^{-3} for ordinary least-squares. These results reveal that the proposed approach reduce the quadratic estimation error and offers improvement over the least squares method leading to more accurate HRF estimation from fNIRS data.

4.2. Real data

After approval of the study protocol by the Stanford University Institutional Review Board, written informed consent was obtained from each participant to participate in this study. The aim of the experiment was to investigate the dynamics of oxygenated and deoxygenated hemoglobin during a motor activity. The experiment was performed on ten healthy young adults (mean age 26.9, four males) who performed a finger-tapping task with no head motion (FO), finger tapping with small head motion (FS) and finger tapping with big head motion (FB). Each finger tapping task consisted of 10 alternating tapping and resting epochs. Each tapping epoch lasted 10 s and each resting epoch lasted 20 s. Before the start of the experiment, participants were asked to sit relaxed and let their right hand rest naturally on their right knee. When the word "Tap" appeared on the screen, they began tapping all four fingers on their right hand at a rate of 3-4 taps/s till a cue on the screen alerted them to stop. Further details of the experiment can be found in [1].

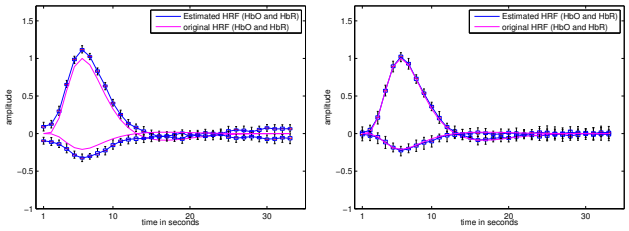

Fig. 1. Estimated HRFs using ordinary least squares method for drifted HbO and HbR fNIRS time-series for σ_ϵ^2 = 0.05 (left). Estimated HRFs using proposed method for drifted HbO and HbR fNIRS time-series for σ_ϵ^2 = 0.05 (right)

In this study, we investigated the FS-FB blocks for the concentration change of HbO and HbR for one of the subjects. In these blocks, apart from the finger tapping task, further event-related instructions were given to the participants to move their head in the indicated directions (forward, left, backward and right) supplemented either by "small" for FS-block or "big" for FB-block while kept on performing the tapping task. Each of the four motion instruction occurred 10 times within each block, on average every 9 s (1 s standard deviation) asynchronous with the alternating finger tapping and resting epochs. For "big" head motions, participants were asked to move their head as far as possible without moving their shoulders; for "small" head motions, they were asked to move half way. Furthermore, they were asked to move their head at a natural speed.

The concentration change of HbO and HbR was measured using ETG-4000 (Hitachi Medical, Japan) Optical Topography system with a sampling frequency of 10 Hz and characterizing wavelengths in the range (695-830 nm). Two 4x4 measurement patches (each 24 channels) provided by Hitachi were used to measure the task-related hemodynamics activity. For the expected activation in the left motor cortex by the known right hand finger tapping task, the patches were attached to a

swimming cap in a manner that covered the bilateral motor cortex of each subject.

The resulting activated HbO and HbR signals from the left motor cortex were approached for HRF estimation with both the ordinary least squares and the proposed method. Results are shown in Figure 2 for two of the channels with different HbO and HbR hemodynamics triggered by underlying neuronal activity in the left motor cortex of the brain. In comparison to ordinary least squares, the proposed method is well-adapted to correctly estimate the two different qualitative measures from real fNIRS data.

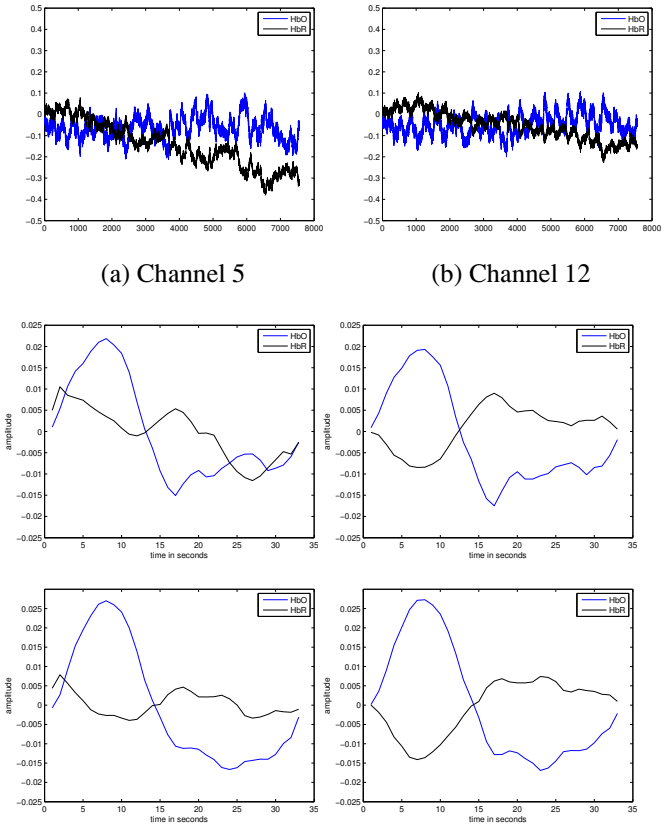

(a) Channel 5 (b) Channel 12

(c) least squares (d) proposed method

Fig. 2. a-b) acquired real fNIRS time-series. Black represent HbR, Blue represent HbO. c) Estimated HRFs using ordinary least squares method for channel 5 (top) and channel 12 (bottom) d) Estimated HRFs using proposed method for channel 5 (top) and channel 12 (bottom)

5. CONCLUSION

In this paper we have proposed a simple, reliable and effective nonparametric HRF estimation procedure using the linear least square estimator. Its implementation is easy and avoids the selection of nuisance covariates [14][12] or their estimation [18]. The proposed method is based on a first order differencing method. Using this HRF estimate, the baseline drift can be estimated using a wavelet thresholding technique applied to the residuals obtained by removing the estimated induced activation response from the fNIRS times series. The derived HRF estimate is proven to be consistent. The effectiveness and performance of the proposed HRF estimation procedure was illustrated on simulated data and tested on real fNIRS data.

Appendix

For $j = 1, ..., N-1$, (4)

$$y_{i,j+1} - y_{i,j} = (X_{j+1} - X_j)\theta_i + f_i(t_{j+1}) - f_i(t_j) + e_{i,j}, \quad (9)$$

can be written in a vector form

$$\mathbf{d}_i = R\theta_i + \mathbf{g}_i + \mathbf{e}_i \quad (10)$$

where $\mathbf{d}_i = (y_{i,2} - y_{i,1}, ..., y_{i,N} - y_{i,N-1})^\top$ is an $(N-1) \times 1$ vector, $R = [X_2 - X_1; ...; X_N - X_{N-1}]^\top$ is an $(N-1) \times p$ matrix, $\mathbf{g}_i = (f_2 - f_1, ..., f_N - f_{N-1})^\top$ is an $(N-1) \times 1$ vector and $\mathbf{e}_i = (\epsilon_2 - \epsilon_1, ..., \epsilon_N - \epsilon_{N-1})^\top$ is an $(N-1) \times 1$ vector.

From (6), we have

$$(R^\top R)^{-1} R^\top \mathbf{z}_i = \theta_i + (R^\top R)^{-1} R^\top \mathbf{g}_i + (R^\top R)^{-1} R^\top \mathbf{e}_i. \quad (11)$$

We use the following asymptotic identifiability assumptions:

A1- The matrix

$$C_N = \frac{1}{N} \sum_{j=1}^{N-1} (X_{j+1} - X_j)^\top (X_{j+1} - X_j) = \frac{1}{N} R^\top R$$

converge toward an invertible matrix C.

A2- The function $\mathbf{f}$ is Lipschitz continuous.

The central limit theorem induces the asymptotic normality of the terms $\sqrt{N}(R^\top R)^{-1} R^\top \mathbf{e}_i$. Its mean is given by

$$E\left(\sqrt{N}(R^\top R)^{-1} R^\top \mathbf{e}_i\right) = 0$$

and the covariance is

$$E\left(N(R^\top R)^{-1} R^\top \mathbf{e}_i \mathbf{e}_i^\top R (R^\top R)^{-1}\right) = \sigma_\epsilon^2 C^{-1}$$

Using assumption A2, the first moment of the second term of (11) is of order

$$E\left(\sqrt{N}(R^\top R)^{-1} R^\top \mathbf{g}_i\right) = O\left(\frac{1}{N}\right) \quad (12)$$

and using Cauchy-Schwartz inequality its variance is of order

$$E\left(N(R^\top R)^{-1} R^\top \mathbf{g}_i \mathbf{g}_i^\top R (R^\top R)^{-1}\right) = O\left(\frac{1}{N^2}\right) \quad (13)$$

Therefore for sufficiently large N, we have $\sqrt{N}(\hat{\theta}_i - \theta_i) \to N(0, \sigma_\epsilon^2 C^{-1})$.

6. REFERENCES

[1] X. Cui, S. Bray, and A. L. Reiss, "Functional near infrared spectroscopy (NIRS) signal improvement based on negative correlation between oxygenated and deoxygenated hemoglobin dynamics," *Neuroimage*, vol. 49, pp. 3039–3046, 2010.

[2] G. R. Wylie, H. Graber, G. T. Voelbel, A. D. Kohl, J. DeLuca, Y. Pei, Y. Xu, and R. L. Barbour, "Using co-variations in the Hb signal to detect visual activation: A near infrared spectroscopic imaging study.," *Neuroimage*, vol. 47(2), pp. 473–481, 2009.

[3] D. Malonek and A. Grinvald, "Interactions between electrical activity and cortical microcirculation revealed by imaging spectroscopy: implications for functional brain mapping.," *Science*, vol. 272, pp. 551–554, 1996.

[4] A. Villringer and B. Chance, "Non-invasive optical spectroscopy and imaging of human brain function," *Trends Neurosci.*, vol. 20, pp. 435–442, 1997.

[5] J. M. Lina, C. Matteau-Pelletier, M. Dehaes, M. Desjardins, and F. Lesage, "Wavelet-based estimation of the hemodynamic responses in diffuse optical imaging.," *Med. Inage Anal.*, vol. 4, pp. 606–616, 2010.

[6] M. M. Plichta, S. Heinzel, C. Ehlis, P. Pauli, and A.J. Fallgatter, "Model-based analysis of rapid event-related functional near-infrared spectroscopy (NIRS) data: A parametric validation study.," *Neuroimage*, vol. 35, pp. 625–634, 2007.

[7] G. M. Boynton, S. A. Engel, G. H. Glover, and D. J. Heeger, "Linear systems analysis of functional magnetic resonance imaging in human v1," *The Journal of Neuroscience*, vol. 16, pp. 4207–4221, 1996.

[8] J. Gonzalez-Castillo, Z. S. Saad, D. A. Handwerker, S. J. Inati, N. Brenowitz, and P. A. Bandettini, "Whole-brain, time-locked activation with simple tasks revealed using massive averaging and model-free analysis," *PNAS*, vol. 109, pp. 5487–5492, 2012.

[9] A. K. Seghouane and S. I. Amari, "Identification of directed influence: Granger causality, kullback-leibler divergence and complexity," *Neural Computation*, vol. 24, pp. 1722–1739, 2012.

[10] J. Cohen-Adad, S. Chapuisat, J. Doyon, Rossignol, J.-M. Lina, H. Benali, and F. Lesag, "Activation detection in diffuse optical imaging by means of the general linear model," *Medic. Image Anal.*, vol. 11, pp. 616–629, 2007.

[11] M. S. Cohen, "Parametric analysis of fMRI data using linear systems methods," *NeuroImage*, vol. 6, pp. 93–103, 1997.

[12] G. Marrelec, P. Ciuciu, , M. Pelegrini-Issac, and H. Benali, "Estimation of the hemodynamic response in event related functional MRI: Bayesian networks as a framework for efficient Bayesian modeling and inference," *IEEE Transactions on Medical Imaging*, vol. 23, pp. 959–967, 2004.

[13] G. H. Glover, "Deconvolution of impulse response in event-related BOLD fMRI," *Neuroimage*, vol. 9, pp. 416–429, 1999.

[14] S. Makni, J. Idier, and J. B. Poline, "Joint detection-estimation of brain activity in functional MRI: A multichannel deconvolution solution," *IEEE Transactions on Signal Processing*, vol. 53, pp. 3488–3502, 2005.

[15] F. G. Meyer, "Wavelet-based estimation of a semiparametric generalized linear model of fMRI time series," *IEEE Transactions on Medical Imaging*, vol. 22, pp. 315–322, 2003.

[16] T. W. Anderson, *The Statistical Analysis of Time Series*, Wiley New York, 1971.

[17] A. Yatchew, "An elementary estimator of the partial linear model," *Economics Letters*, vol. 57, pp. 135–143, 1997.

[18] A. K. Seghouane and A. Shah, "HRF estimation in fMRI data with unknown drift matrix by iterative minimization of the Kullback-Leibler divergence," *IEEE Transactions on Medical Imaging*, vol. 2, pp. 192–206, 2012.

[19] A. K. Seghouane and M. Bekara, "A small sample model selection criterion based on the Kullback symmetric divergence," *IEEE Transactions on Signal Processing*, vol. 52, pp. 3314–3323, 2004.

[20] A. K. Seghouane and S. I. Amari, "The AIC criterion and symmetrizing the Kullback-Leibler divergence," *IEEE Transactions on Neural Networks*, vol. 18, pp. 97–106, 2007.

[21] A. K. Seghouane, "Asymptotic bootstrap corrections of AIC for linear regression models," *Signal Processing*, vol. 90, pp. 217–224, 2010.

[22] S. Mallat, *A wavelet tour of signal processing*, Academic Press, Dec. 2008.

[23] K. J. Friston, A. P. Holmes, J. Ashburner, and J. B. Poline, *SPM8*, http://www.fil.ion.ucl.ac.uk/spm/.

[24] S. Coyle, T. Ward, and C. Markham, "Physiological noise in near-infrared spectroscopy: implications for optical brain computer interfacing.," *IEEE Eng. Med. Biol. Soc.*, pp. 4540–4543, 2004.